

Hybrid infrared with hot air drying of Pisang-Awak banana: Kinetics and shrinkage quality

Kritsada Puangsuwan¹ | Saysunee Jumrat^{1,2} | Jirapond Muangprathub^{1,2} |
Teerask Punvichai^{2,3} | Seppo Karrila¹ | Yutthapong Pianroj^{1,2} 

¹Faculty of Science and Industrial Technology, Prince of Songkla University, Surat-Thani Campus, Suratthani, Thailand

²Integrated High-Value of Oleochemical (IH-VO) Research Center, Prince of Songkla University, Surat-Thani Campus, Suratthani, Thailand

³Faculty of Innovation Agriculture and Fisheries Establishment Project, Prince of Songkla University, Surat-Thani Campus, Suratthani, Thailand

Correspondence

Yutthapong Pianroj, Faculty of Science and Industrial Technology, Prince of Songkla University, Surat-Thani Campus, Muang, Suratthani 84000, Thailand.
Email: yutthapong.p@psu.ac.th

Funding information

Prince of Songkla University, Surat Thani Campus; Research and Development Office, Prince of Songkla University

Abstract

The purpose of this study was to develop the prototype drying system for drying the Pisang-Awak (PA) banana. It was designed and implemented to study the drying kinetics in each drying mode: hot air drying (HA), infrared drying (IR), and hybrid drying (Hy). The experimental results were fit with simulation results from the finite element method (FEM). Two statistical parameters, the coefficient of determination (R^2) and the root mean square error (RMSE), were used to assess the fit between experimental results and simulation results, and their respective ranges were 0.960–0.997 and 0.014–0.050. For PA banana drying the most suitable drying mode is hybrid, combining 1.5 m/s flow of hot air and IR heating at 60°C drying temperature. The axial and radial shrinkages of PA banana were the largest in Hy mode at 60°C, namely 18.2 and 27.3%, respectively, and this choice gave the best/lowest specific energy consumption (SEC) for drying performance and the best final dried PA banana.

Practical Applications

The understanding of the drying kinetics and shrinkage properties of the dried PA banana is important for the choice of drying process because these reflect the quality of the dried product and help an engineer to design the drying system. Therefore, the empirical mathematical modeling of the drying process serves a crucial role in the food industry sector. These results can be used to quantify temperature and moisture content as functions of drying time to monitor the drying process of PA banana, saving energy and time.

1 | INTRODUCTION

In the years 2017–2019, the top three produced bananas in Thailand were Pisang-Awak (PA) banana, Banana, and Pisang-Mas banana, at respectively 3,993, 903, and 670 ktons (Department of Agricultural Extension, n.d.). The PA banana is an economic plant widely used in Thai dessert recipes. Consuming two such bananas can give enough energy for up to 90 min of exercise, with also large doses of dietary fiber, vitamins, and minerals. Benefits of bananas to the human body include reducing bad breath, providing anti-oxidants, and relief to constipation, morning sickness, hemorrhoids, obesity, high blood pressure, broken capillaries, and so on (Robinson & Galan Sauco, 2011).

Growing bananas gives year-round production in Thailand, but in some seasons the production can exceed the demand, while the shelf life of bananas is only 5 to 7 days before spoilage by the enzymes in them (Naknaen, Charoenthaikij, & Kerdsup, 2016; Sankat & Castaigne, 2004). Processing banana is an alternative way to address this problem.

Drying is one way to preserve food products for prolonged storage. It removes water or moisture under controlled conditions by the use of heat. The low moisture level then inhibits the growth of harmful microbes, inactivates enzymes, and helps avoid toxins, parasites, and various insects (Bala, Mondol, Biswas, Das Chowdury, & Janjai, 2003). The design of a drying system requires the use of

engineering principles for heat and mass transfer within the bananas, occurring simultaneously to evaporate moisture that exits at the banana surface. The mode of heat transmission into bananas may be by conduction, convection, or radiation. From a literature review on drying food products, there are many methods, each with its advantages and disadvantages. Solar drying is clean and uses free energy from nature, but the solar radiation intensity depends on the weather, being unpredictable and low intensity, so it takes a long time to dry in the sunlight, and the quality of the product is not well controlled (Bala et al., 2003; Condorí, Echazú, & Saravia, 2001; Jain & Pathare, 2007; Janjai & Tung, 2005). Microwave drying methods are interesting, but electromagnetic high-frequency irradiation can be harmful to living things and safety aspects must be addressed (Puangsuwan et al., 2021; Sungsoontorn, Jumrat, Pianroj, & Rattanadecho, 2016). Hot air drying (HA) uses convection of heat to expel the moisture from bananas, and this requires high energy input. But the drying efficiency is low because the moisture evaporation rate on the surface is faster than the moisture diffusion rate within the banana to the surface, causing the skin to dry and harden, and hinder the passage of moisture. Therefore, the porous texture of the bananas will have a significant amount of moisture remaining, resulting in decreased quality of the dried products (Chua & Chou, 2003; Tirawanichakul, Na Phatthalung, & Tirawanichakul, 2008). In addition, infrared drying (IR) can effectively penetrate the banana structure. Infrared waves are electromagnetic field energy that moves at the speed of light impacting polar molecules (water) and transforming into heat energy instantly. The temperature within the banana can then be higher than at its surface (Glouannec, Lecharpentier, & Noel, 2002; Sakai & Hanzawa, 1994). It was found that after drying, the skin of bananas did not become wrinkled and remained at the same quality as before drying (Ning & Han, 2013). In addition, infrared waves provide fast and consistent heating. The system is easy to install, saves energy, and shortens drying time (Chua & Chou, 2003; Dondee, Meeso, Soponronnarit, & Siriamornpun, 2011). The use of suitable drying techniques for bananas can lead to a product with a light color, soft consistency, and pleasant taste and aroma. The structure inside PA banana is a non-porous solid material, so the moisture content relates to the structure while it is dried and there will not be a constant drying rate period like there would be with free water in connected pore space (de Lima, Farias Neto, & Silva, 2012; de Lima, Queiroz, & Nebra, 2002). In many previous studies (de Souza, de Andrade, & Rios, 2019; Farias et al., 2020; Maskan, 2000; Rahman, Ahmed, & Islam, 2018; Smitabhindu, Janjai, & Chankong, 2008; Thuwapanichayanan, Prachayawarakorn, & Soponronnarit, 2008), the drying of PA bananas has stopped microorganism activity when the final moisture content of PA banana is below 13%w.b.; moreover, temperature and drying time are important parameters that affect the physical structure after drying.

Therefore, in this study, we designed and implemented a prototype system for Pisang-Awak banana drying, which can operate in three drying modes: HA, IR, or both HA and IR, here named hybrid drying (Hy). The function and performance of the system are described in the next section. In Section 3, the experimental results of

drying kinetics are fit with simulation results from finite element software. Finally, the last section assesses results on drying shrinkage of the PA banana, and the specific energy consumption (SEC), and these are compared between the drying mode alternatives.

2 | MATERIALS AND METHODS

2.1 | Drying system

In this study, a prototype system for PA banana drying was developed. It had two types of heat sources: one is a heater with an air fan that can adjust flow speed in ventilation of HA, and the other heat source is an infrared tube, so this system can operate in three modes of drying. The first is HA, the second is IR, and the last one is Hy that combines HA and IR. The prototype was made of stainless steel to dimensions $64 \times 54 \times 75 \text{ cm}^3$, and it can maintain elevated temperature in the chamber with insulation between the aluminum sheets on the insides and outsides of the walls. The prototype system is shown in Figure 1.

The main and controller components of the PA banana drying system are shown in Figure 2. In this figure, the input part is analog signals from all sensors, and user commands are entered with a keypad. Then, all signals from analog inputs and the power supply are processed by the main processor part, and the response commands are sent to control and displayed by the output part. There are two heat-generating sets. The first set is a convection heat source providing hot air from a 1,000 W coil heater and uses 220 V_{AC}, 0.3 A fans. This set is installed on the side of the drying system and blows hot air to the system. The second heat source radiates heat from two 500 W infrared heaters installed 17 cm above each tray for bananas. Moreover, the chamber control system is equipped with a DS18B20 temperature and an AM2301 humidity sensor, and these send digital signals to the Arduino Mega2560 microcontroller (MCU). This system controls the operation of the heater and ventilation fans to maintain

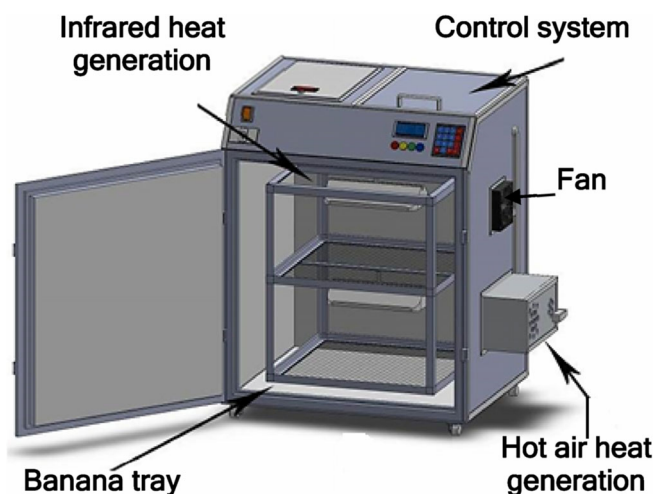


FIGURE 1 The prototype system for Pisang-Awak banana drying

the temperature and relative humidity conditions in the chamber as specified during drying, while the bananas are weighed by a load cell through the axis attached to the banana trays, and the analog signal is passed through the HX711 module that amplifies it. The banana weight data are analyzed for the moisture content in the bananas using the AOAC standard method (AOAC, 2005) through microcontroller processing, and the result is recorded to the memory card every 15 min.

The prototype drying system enables the drying modes with convection (HA), IR, and Hy combining both convection and infrared. For convection heating, the system has two alternative airflow rates namely 1.5 and 2.5 m/s. To verify the performance of the drying system, various conditions (HA at 1.5 m/s, HA at 2.5 m/s, IR, Hy at 1.5 m/s, and Hy at 2.5 m/s) were tested with temperature setpoints 50, 60, and 70°C, and the results are shown in Figure 3a–c, respectively. In this figure, the system increases the temperature from

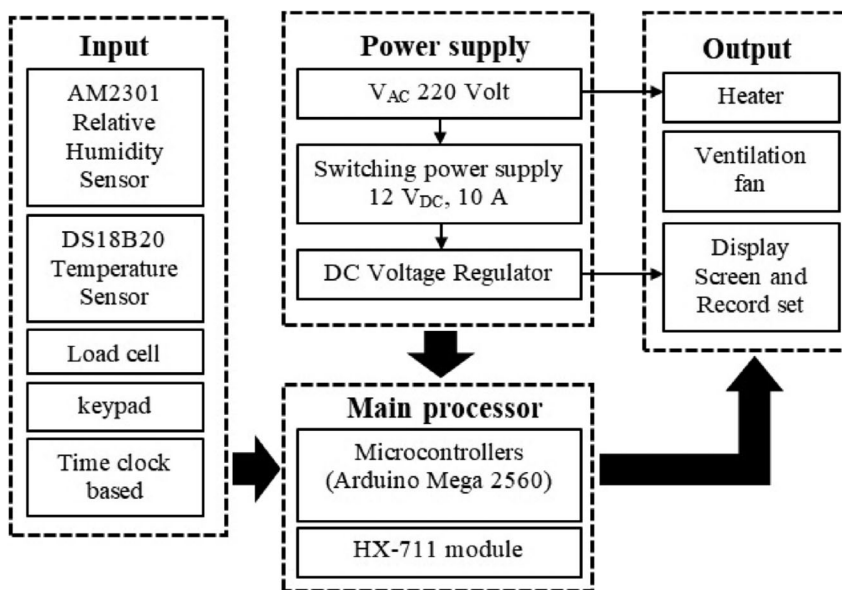


FIGURE 2 Controller diagram for the Pisang-Awak banana drying system

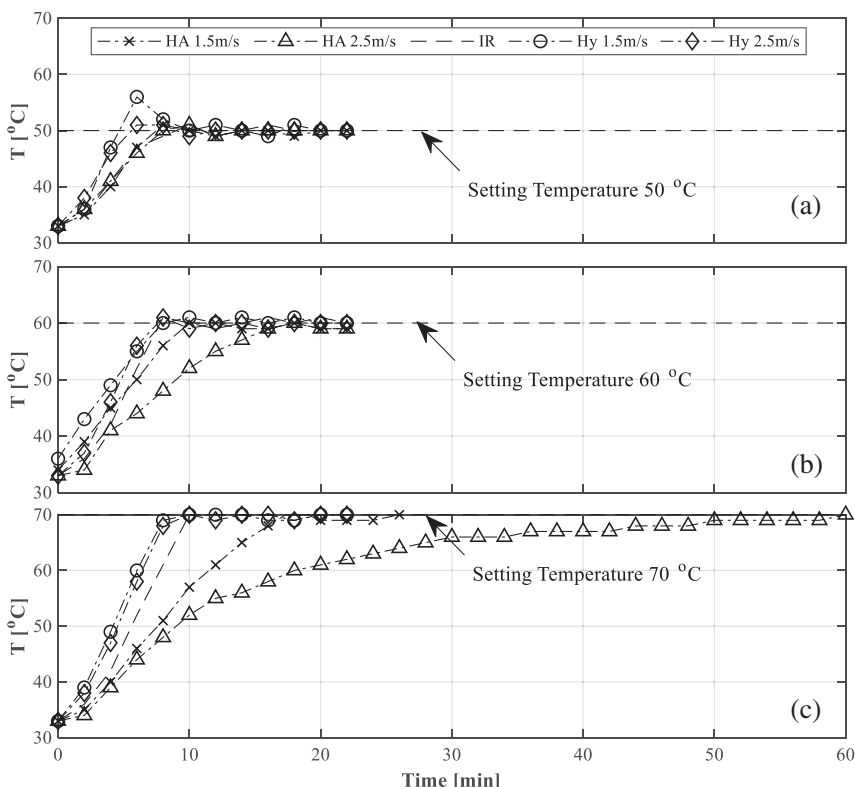


FIGURE 3 Performance testing of the drying system at different temperature settings: (a) 50°C, (b) 60°C, and (c) 70°C

ambient to the targeted setpoint in around 10 min and then maintains the target temperature for the testing period. The airflow rate at 1.5 m/s gives a high heating rate while consuming less energy than airflow rate 2.5 m/s, so the airflow rate 1.5 m/s was used for convection drying in the remainder of this study. The reason for this phenomenon is the heat balance between cumulative heat inside the drying cavity, and the airflow rate at 1.5 m/s, which carries heat and atmospheric drying air outside the drying cavity. This evidence is shown in Figure 3, in which the case of Hy at 1.5 m/s gave the best heating rate with the steepest slope in the graph.

2.2 | Sample preparation and drying kinetics study

The ripe PA banana samples were used in ripeness stage 6 of the 8 stages, at which the skin color is yellow on the entire banana. The bananas were peeled and measured for average thickness and length, which were 2.84 ± 0.28 cm and 8.49 ± 0.78 cm, respectively. After that, the initial moisture content of bananas was determined gravimetrically using the AOAC standard method (AOAC, 2005), and the PA banana sample was dried with the drying system at setpoint temperatures 50, 60, and 70°C for each drying mode. Three drying modes were all used to study the drying kinetics. The first mode is HA, which has a hot air velocity 1.5 m/s. The second is IR, and the final mode is Hy combining HA and IR. The PA banana samples were dried until the final moisture content of the bananas was 13%w.b. (MR = 0.2) ($n = 3$ replicates) (Farias et al., 2020; Nguyen & Price, 2007). The moisture content is defined as the percentage on wet basis (%w.b.). It can be determined as in Equation (1).

$$\%w.b. = \left(\frac{W_a - W_b}{W_a} \right) \times 100, \quad (1)$$

where W_a is the weight of PA banana before drying (g) and W_b is the weight of PA banana after drying (g). Then the moisture ratio (MR) of PA banana is calculated using this equation:

$$MR = \frac{M_t - M_e}{M_0 - M_e}, \quad (2)$$

where M_t is the moisture content at a given time, M_0 is the initial moisture content, and M_e is the equilibrium moisture content. For a long drying time, the value of M_e is relatively small compared to M_t or M_0 , thus, Equation (2) can be simplified to $MR = M_t/M_0$ (Puangsuwan et al., 2021; Puangsuwan, Chongcheawchamnan, & Tongura, 2015; Salehi, Kashaninejad, & Jafarianlari, 2017; Tunckal & Doymaz, 2020). The simulation results, which are based on the finite element method (FEM), were fit to the experimental drying curves (MR vs. drying time). Therefore, to assess the goodness of fit, the coefficient of determination (R^2) and root mean square error (RMSE) (Kaveh, Golpour, Gonçalves, Ghafouri, & Guiné, 2021; Kipcak & Doymaz, 2020a) were used as indicators of model performance, and the RMSE can be calculated as follows:

$$RMSE = \sqrt{\frac{1}{N} \sum_{i=1}^N (MR_{sim,i} - MR_{exp,i})^2}, \quad (3)$$

where $MR_{exp,i}$ and $MR_{sim,i}$ refer to the experimental and simulation dimensionless moisture ratios, respectively, and N is the number of data points. As indicators for goodness of fit, a larger R^2 is better, while a smaller RMSE is better (Chen et al., 2015; Chen, Li, & Zhu, 2012; Pianroj, Werapun, Inthapan, Jumrat, & Karrila, 2018; Wang et al., 2007).

2.3 | Simulation set-up

PA banana was modeled as a straight circular finite cylinder of 1.49 cm radius (R) and 8.49 cm height (L). The diffusion was assumed axially symmetric, so a 2-D model in the commercial COMSOL Multiphysics simulation software package was used to simulate the moisture profiles during drying of a PA banana, with the element grid shown in Figure 4.

The FEM is a powerful numerical analysis approach to simulation by solving partial differential equation models, and many kinds of scientific and engineering problems can be solved approximately by extending conventional models for one type of physics into multiphysics models that involve coupled physics phenomena. In the current simulations, there are time-dependent interfaces with state defined by temperature and moisture concentration. The multiphysics model for HA combines *heat transfer in solids (ht)* and *transport of*

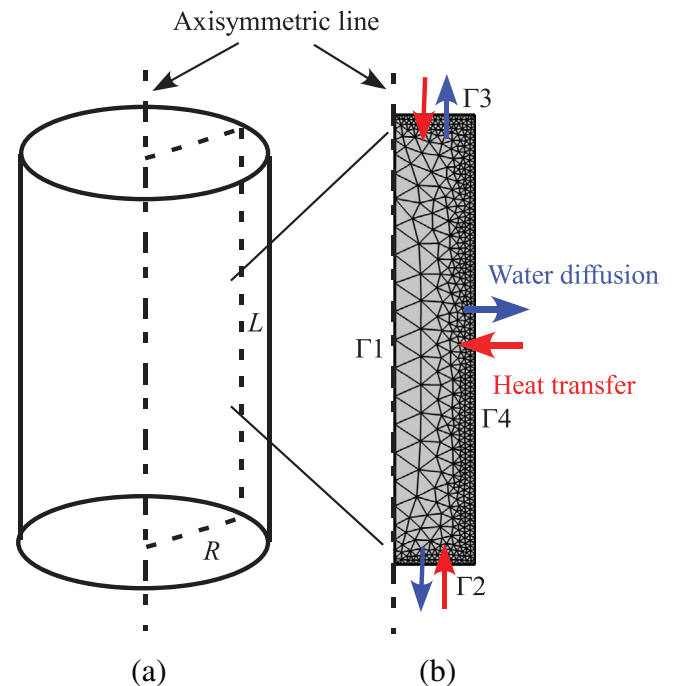


FIGURE 4 (a) The finite cylinder (radius R and height L) and (b) the non-uniform FEM mesh. Numbers on (b) label the boundaries of the model for specification of the boundary conditions

diluted species (tds) submodel types. It should be noted that for these simulation models, the convective velocity field outside the sample was given by the coefficients for convective heating and moisture transfer to the surrounding air, and diffusive processes describe both heat and moisture transport inside the banana. The general Fourier's law of heat transfer and Fick's law of mass transfer in an axisymmetric case are shown as Equations (4) and (5), respectively.

$$\rho C_p \frac{\partial T}{\partial t} = k \left[\frac{1}{r} \frac{\partial}{\partial r} \left(r \frac{\partial}{\partial r} + \frac{\partial^2 T}{\partial z^2} \right) \right], \quad (4)$$

$$\frac{\partial c}{\partial t} = D \left[\frac{1}{r} \frac{\partial}{\partial r} \left(r \frac{\partial c}{\partial r} + \frac{\partial^2 c}{\partial z^2} \right) \right], \quad (5)$$

where ρ , C_p , k , r , z , t , c , D are density (kg/m^3), specific heat ($\text{J kg}^{-1} \text{K}^{-1}$), thermal conductivity ($\text{W m}^{-1} \text{K}^{-1}$), banana radius (m), banana thickness (m), drying time (s), moisture concentration (mol/m^3), and the moisture diffusion coefficient (m^2/s), respectively. For initial conditions, we assumed that the temperature and moisture concentration in a banana are uniform before drying, equal to T_0 and c_0 , as shown in Equation (6). Moreover, the temperature field on boundaries 1 is symmetric, while boundaries 2, 3, and 4 receive air convection heat, so the heat flux out of the banana due to moisture vaporization on these boundaries is shown in Equations (7) and (8), respectively. The boundary conditions for moisture diffusion are shown in Equations (9) and (10).

$$T = T_0, c = c_0, t = 0, 0 \leq r \leq R \quad (6)$$

$$\hat{n} \cdot (-k \nabla T) = 0; \text{ at } \Gamma_1 \quad (7)$$

$$\hat{n} \cdot (-k \nabla T) = h_T (T_{\text{air}} - T) + \lambda \hat{n} \cdot (D \nabla c); \text{ at } \Gamma_2, \Gamma_3, \text{ and } \Gamma_4 \quad (8)$$

$$\hat{n} \cdot (-D \nabla c) = 0; \text{ at } \Gamma_1 \quad (9)$$

$$\hat{n} \cdot (D \nabla c) = k_c (c_b - c); \text{ at } \Gamma_2, \Gamma_3, \text{ and } \Gamma_4, \quad (10)$$

where \hat{n} is the unit vector pointing outward from the boundaries, and h_T is the heat transfer coefficient ($\text{W m}^{-2} \text{K}^{-1}$) calculated from Seyedabadi, Khojastehpour, and Abbaspour-Fard (2017) and Singh and Heldman (2014), T_{air} is the oven air temperature, k_c refers to the mass transfer coefficient (m/s), λ is the latent heat of moisture evaporation (J/kg), given as a function of temperature in Equation (11) (Seyedabadi et al., 2017), and c_b is the outside air moisture concentration (mol/m^3).

$$\lambda = 2,501.05 \times 10^3 \left(\frac{647.3 - T}{647.3 - 273.15} \right)^{0.3298}. \quad (11)$$

In the case of IR and Hy, a further boundary condition, named *surface-to-surface radiation (rad)*, was included to describe the radiation transfer of heat from an IR source. The total incoming and outgoing

radiative fluxes at boundaries 2, 3, and 4 are called irradiation (G) and radiosity (J), respectively. The radiosity is the sum of diffusively reflected and emitted radiation:

$$J = \rho_d G + \varepsilon \sigma T^4, \quad (12)$$

where ε is emissivity, $\rho_d = 1 - \varepsilon$ is the diffuse reflectivity, σ is the Stefan-Boltzmann constant, and T is temperature. All the parameters used in this study are shown in Table 1. By solving the moisture concentration (c) in Equation (5), the conversion to moisture concentration of the mass fraction of water (x_w) inside PA banana or MR can be done with Equation (13) (COMSOL, n.d.).

$$c = \frac{x_w \times \rho}{M_{\text{H}_2\text{O}}}, \quad (13)$$

where $M_{\text{H}_2\text{O}}$ is the molecular weight of water (18 g/mol) and x_w is mass fraction of water.

2.4 | Specific energy consumption and shrinkage of PA banana

The SEC indicates the performance of a drying system. It is the amount of energy supplied to the system that is required to remove 1 g of water from the dried material, so that SEC can be calculated from Jindarat, Rattanadecho, and Vongpradubchai (2011) and Tirawanichakul et al. (2008)

$$\text{SEC} \equiv \frac{Q_i}{W_{\text{loss}}}, \quad (14)$$

where Q_i is the total energy supplied into the drying system (kJ) and W_{loss} is the water loss from the drying material (g). In this work, the input of electrical energy will be supplied to the PA banana drying

TABLE 1 Simulation parameters applied in the model

Parameter (notation)	Unit	Value
Density of PA banana (ρ) (Seyedabadi et al., 2017)	kg/m^3	1,250
Thermal conductivity of PA banana (k) (Seyedabadi et al., 2017)	W/(m K)	0.40
Specific heat of PA banana (C_p) (Seyedabadi et al., 2017)	J/kg K	2,600
Mass transfer coefficient (k_c) (Seyedabadi et al., 2017)	m/s	12.06×10^{-8}
Air moisture concentration (c_b) (Chen, Marks, & Murphy, 1999)	mol/m^3	1.39
Moisture diffusion coefficient (D) (da Silva, e Silva, & Gomes, 2013)	m^2/s	1.49×10^{-8}
Surface emissivity of PA banana (ε)	-	0.55

Abbreviation: PA, Pisang-Awak.

system, which transforms the input energy to other forms of energy such as heat from heater and infrared tubes, and also to airflow from ventilation fans. For monitoring the input energy consumption, a clamp meter (model UT200A) was run from start to finish of the drying period (final moisture content 13%w.b. or MR 0.2).

The axial shrinkage (A_{sh}) and radial shrinkage (R_{sh}) of fresh PA banana are defined in Equations (15) and (16) (Seyedabadi et al., 2017) based on measuring the changes in thickness (W) and length (L). This was done using a digital Vernier caliper (model 101-2601) as shown in Figure 5 (Barat, Fito, & Chiralt, 2001)

$$\%A_{sh} = \left(\frac{L_i - L_f}{L_i} \right) \times 100 \quad (15)$$

$$\%R_{sh} = \left(1 - \sqrt{\frac{A_f}{A_i}} \right) \times 100, \quad (16)$$

where L_i is the initial length of fresh PA banana before drying (cm), L_f is the final length of fresh PA banana after drying (cm), A_i is the initial surface area (cm²), and A_f is the final surface area (cm²). It should be noted that the finishing criterion of the drying period was the moisture content of PA banana, dried to 13%w.b. or equivalently to 0.2 MR.

In this study, the cross-section area of PA banana can be assumed to be circular, and also W and L are measured for 12 PA banana

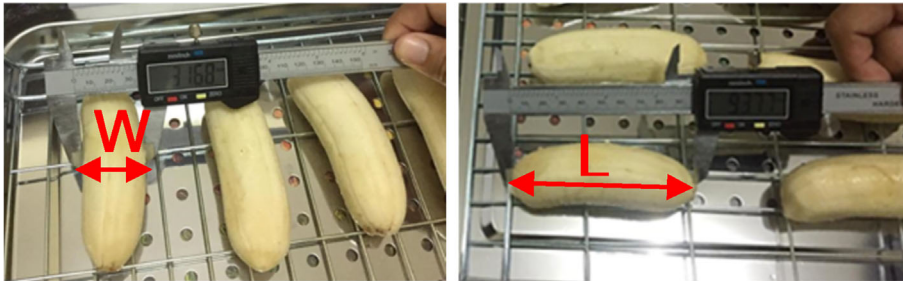


FIGURE 5 Measuring the thickness and length of fresh Pisang-Awak (PA) banana

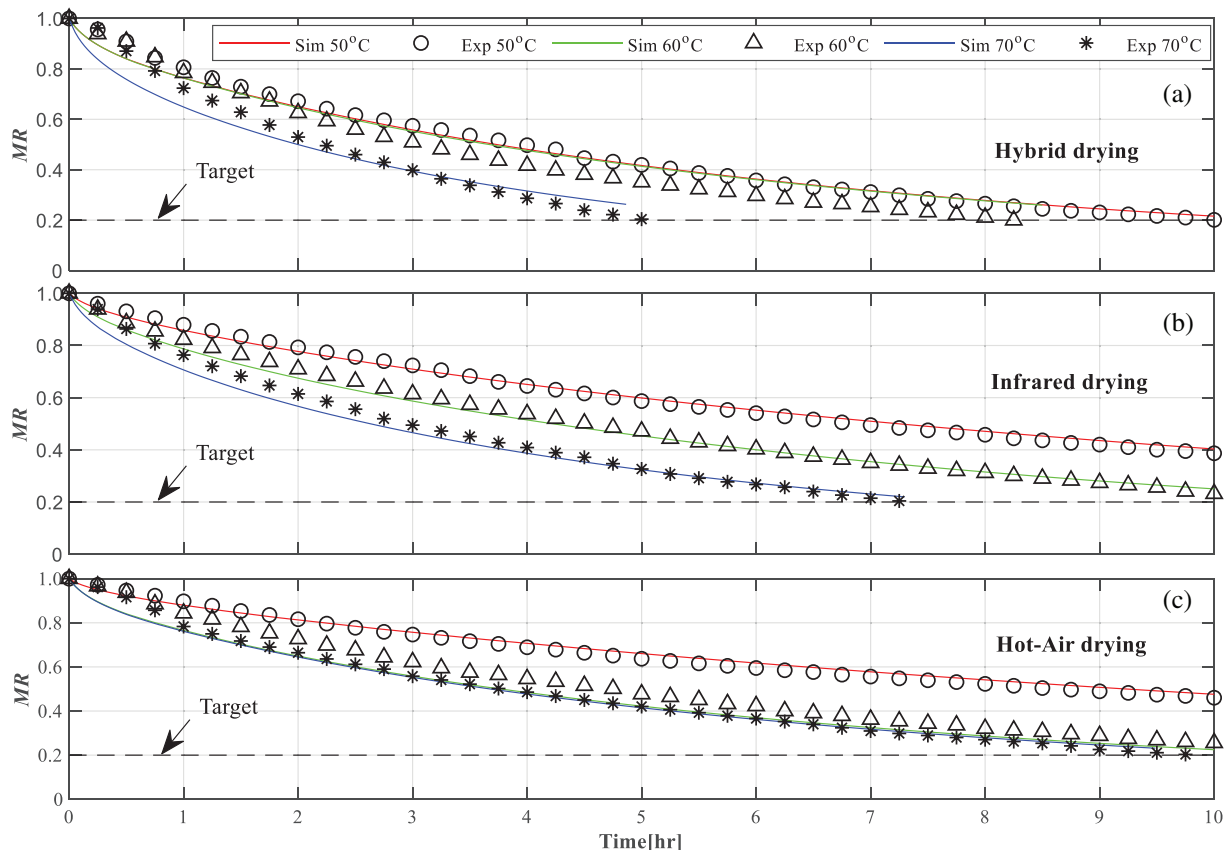
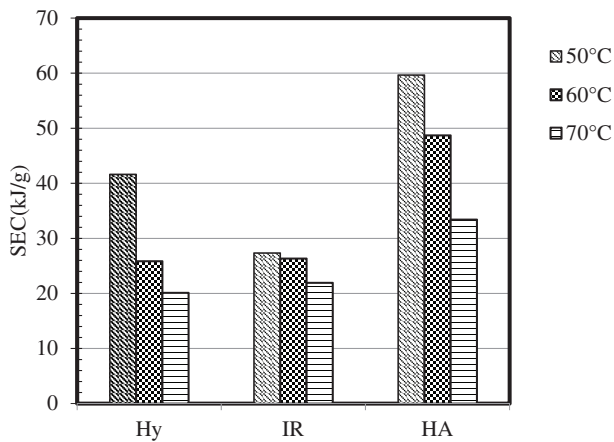


FIGURE 6 Drying kinetics shown by moisture ratio (MR) versus drying time at drying temperatures of 50°C, 60°C, or 70°C with the alternative drying modes: (a) hybrid drying, (b) infrared drying, and (c) hot air drying

TABLE 2 The R^2 and RMSE values for fit of simulation to experimental results

Drying method	50°C		60°C		70°C	
	R^2	RMSE	R^2	RMSE	R^2	RMSE
Hybrid (Hy)	0.994	0.018	0.960	0.049	0.980	0.037
Infrared (IR)	0.992	0.020	0.992	0.020	0.988	0.027
Hot air (HA)	0.996	0.014	0.958	0.050	0.997	0.014

Abbreviation: RMSE, root mean square error.

**FIGURE 7** Specific energy consumption (SEC) on drying Pisang-Awak (PA) banana for all cases tested

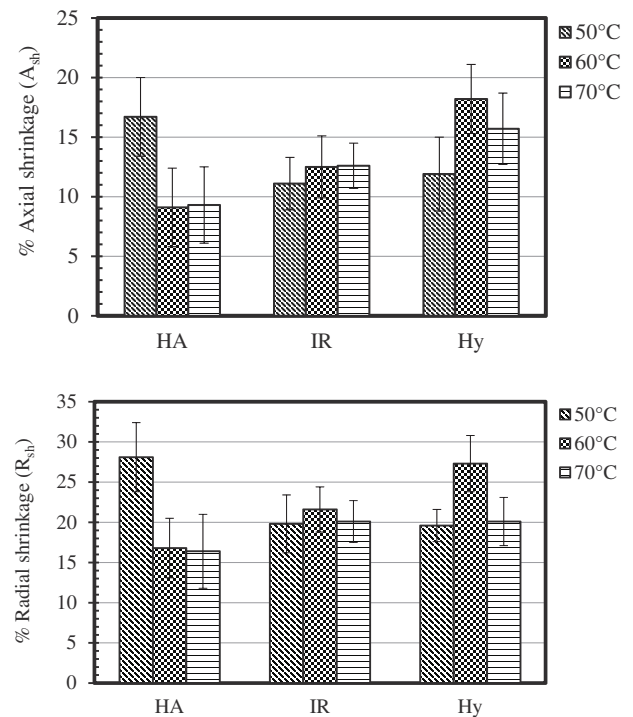
samples per each drying condition studied, and the averages of axial and radial shrinkage will be discussed in the next section.

3 | RESULTS AND DISCUSSION

3.1 | Moisture ratio

The MRs for three different drying temperatures were studied (50, 60, and 70°C) with various drying modes. The first operating mode was HA with an airflow velocity 1.5 m/s. The second was IR, and finally, there was Hy combining HA and IR drying. These were investigated for the drying kinetics of PA bananas. The experimental results and simulation results are plotted in Figure 6.

Figure 6 shows the drying kinetics of PA banana with various temperatures and operating modes of the dryer. No constant drying rate period is seen, instead there was a declining rate throughout the drying period (10 hr). It is found that Hy drying improved heat and mass transport for the specimen inside the oven from those of the other drying modes. The scientific reason for this is the penetration of IR into the specimen. It makes the water molecules in a specimen polarize and align with the electric field of IR. This rapidly increases the heat inside and the added kinetic energy of water molecules moves them to the boundary of the specimen. The temperature difference between inside and outside of the specimen and the forced convection with airflow quickly

**FIGURE 8** The axial ($\%A_{sh}$) and radial ($\%R_{sh}$) shrinkages on drying Pisang-Awak (PA) banana

remove moisture from the boundary of the specimen. The results for Hy are shown in Figure 6a. It is not surprising that a higher drying temperature shortens the drying period to the MR target around 0.2, with a stronger temperature gradient between inside and outside of the specimen. This happens in all drying modes: IR drying in Figure 6b and HA drying in Figure 6c, respectively. Finally, as goodness of fit results, the coefficient of determination (R^2) and the RMSE measure model performance, and are shown in Table 2.

3.2 | Specific energy consumption

The SEC is the amount of electrical energy supplied to the system required to remove 1 g of water from the PA banana during drying, so it reflects the performance of the drying system. It depends on the drying temperature (50, 60, or 70°C) and the drying mode. The least value of SEC indicates the best energy conserving

	Case 1: Effects of drying mode			Case 2: Effects of drying temperature		
	50°C	60°C	70°C	HA	IR	Hy
%A _{sh}	6.23×10^{-5}	4.25×10^{-8}	1.27×10^{-5}	1.09×10^{-6}	0.19	4.99×10^{-5}
%R _{sh}	1.57×10^{-9}	4.90×10^{-8}	0.02	1.56×10^{-9}	0.31	1.19×10^{-7}

Abbreviations: HA, hot air; Hy, hybrid; IR, infrared.



TABLE 3 The *p*-values from one-way ANOVA for checking effects of drying mode and drying temperature

FIGURE 9 The final dried Pisang-Awak (PA) banana from the best drying conditions

performance of the drying system, and SEC results for Hy at drying temperatures 50, 60, and 70°C were 41.62, 25.85 kJ/g, and 20.10 kJ/g, respectively. For IR, the SEC at drying temperatures 50, 60, and 70°C were 27.33, 26.33, and 21.94 kJ/g, respectively. Finally, the SEC results for HA at 50, 60, and 70°C were 59.64, 48.71, and 33.41 kJ/g, respectively. The SEC results are shown in Figure 7, and the energy-based ranking of modes for drying PA banana is Hy, IR, and HA mode, from the best to the worst. However, increasing drying temperature can help moisture evaporation from PA banana and shorten the drying time. This was also found in previous work (Hebbar, Vishwanathan, & Ramesh, 2004; Pan & Atungulu, 2010), in which SEC based drying efficiency decreased in the rank order Hy, IR, and HA, on drying potato, carrot, and similar results in cherry tomatoes were reported by Kipcak and Doymaz (2020b).

3.3 | Shrinkage of Pisang-Awak banana

The shrinkage was calculated in two directions, axial (A_{sh}) and radial (R_{sh}), as described in Equations (15) and (16) of Section 2.4. The overall shrinkage of PA banana was dominantly in the radial direction due to its internal structure, and the heat flux being perpendicular to its surface may have also contributed to this. As shown in Figure 8, the overall %A_{sh} is 13.01 and the overall %R_{sh} is 21.09 across the drying methods and drying temperatures.

To compare the group means statistically a one-way analysis of variance (ANOVA) was run in MS-Excel, with the statistical confidence level set at 95% ($\alpha = 0.05$). Thus, *p*-value < .05 was required to reject the null hypothesis (H_0) and to accept the alternative hypothesis (H_1). Firstly, to determine the effects on %A_{sh} and %R_{sh} by each drying

mode at a fixed drying temperature, H_0 : the mean of %A_{sh} and of %R_{sh} are the same for each drying mode; and H_1 : the mean of %A_{sh} and of %R_{sh} are not the same for the modes. The results are shown in Table 3, Case 1. All *p*-values are less than .05, so the null hypothesis is rejected and the alternative accepted is that there is a mean difference by mode in both %A_{sh} and %R_{sh}. Next, the effect on %A_{sh} and %R_{sh} was tested for each drying temperature at a fixed drying mode. In this case, the hypotheses were H_0 : the mean %A_{sh} and %R_{sh} are the same for all drying temperatures, and H_1 : the means of %A_{sh} and %R_{sh} depend on the drying temperature. The *p*-values are shown in Table 3, Case 2. Most *p*-values are less than .05 except for the IR drying mode that has a *p*-value greater than .05. Therefore, increasing the drying temperature did not effect %A_{sh} and %R_{sh} for the IR drying mode, which is not suitable for drying PA banana. Forced convection is necessary for effecting moisture removal from the boundary of the PA banana (Jamradloedluk, Nathakaranakule, Soponronnarit, & Prachayawarakorn, 2007). In previous works, Seyedabadi et al. (2017) found that %A_{sh} and %R_{sh} of banana samples indicate different shrinkages in axial and radial directions, so they assumed that isotropic shrinkage was no longer valid in their mathematical models. Moreover, they found that both %A_{sh} and %R_{sh} take place in an almost linear pattern for all drying temperatures, and less shrinkage occurs in both axial and radial directions as the drying temperature increases. These observations are in agreement with other studies on drying banana (Prachayawarakorn, Tia, Plyto, & Soponronnarit, 2008), hawthorn fruit (Aral & Beşe, 2016), and pomegranate (Horuz & Maskan, 2015).

In this work, the proper conditions for drying the PA banana used Hy at drying temperature 60°C with %A_{sh} and %R_{sh} on an average 18.2 and 27.3%, respectively, because the final dried PA banana had yellow-brown skin without burns that were seen when drying at

70°C. Final dried PA banana samples from the best drying conditions are shown in Figure 9.

4 | CONCLUSIONS

The prototype system for studying the drying of PA banana was designed, implemented, and tested. It had three modes of drying: HA at airflow 1.5 m/s, IR, and both combined in the Hy operating mode. Each mode was tested with three levels of feedback-controlled drying temperatures: 50, 60, and 70°C. The simulation results calculated with a FEM software package fit the experimental results very well. This was assessed from two statistical parameters, namely R^2 and RMSE, with respective ranges 0.960–0.997 and 0.014–0.050. The best drying mode for PA banana is the combination of HA (at 1.5 m/s) and IR drying, at drying temperature setpoint 60°C, because this gave the best/lowest SEC value for drying performance and the best final dry PA product. Moreover, the axial and radial shrinkages induced by Hy mode at 60°C were the largest among the cases tested, at 18.2 and 27.3%, respectively.

ACKNOWLEDGMENTS

We thank the Research and Development Office, Prince of Songkla University (RDO, PSU) and Prince of Songkla University, Surat Thani Campus for supporting this study under the Integrated High-Value of Oleochemical (IH-VO) Research Center.

AUTHOR CONTRIBUTIONS

Kritsada Puangsuwan: Methodology; project administration; supervision. **Saysunee Jumrat:** Formal analysis; validation. **Jirapond Muangprathub:** Data curation; software. **Teerasak Punvichai:** Investigation; visualization. **Seppo Karrila:** Supervision; writing-review & editing. **Yutthapong Pianroj:** Conceptualization; data curation; methodology; supervision; visualization; writing - original draft.

DATA AVAILABILITY STATEMENT

All data of this study are available from the corresponding author upon reasonable request.

ORCID

Yutthapong Pianroj  <https://orcid.org/0000-0002-4500-1045>

REFERENCES

- AOAC. (2005). *Official methods of analysis* (18th ed.). Washington, DC: Association of Official Analytical Chemists.
- Aral, S., & Beşe, A. V. (2016). Convective drying of hawthorn fruit (*Crataegus* spp.): Effect of experimental parameters on drying kinetics, color, shrinkage, and rehydration capacity. *Food Chemistry*, 210, 577–584. <https://doi.org/10.1016/j.foodchem.2016.04.128>
- Bala, B. K., Mondol, M. R. A., Biswas, B. K., Das Chowdury, B. L., & Janjai, S. (2003). Solar drying of pineapple using solar tunnel drier. *Renewable Energy*, 28(2), 183–190. [https://doi.org/10.1016/S0960-1481\(02\)00034-4](https://doi.org/10.1016/S0960-1481(02)00034-4)
- Barat, J. M., Fito, P., & Chiralt, A. (2001). Modeling of simultaneous mass transfer and structural changes in fruit tissues. *Journal of Food Engineering*, 49(2), 77–85. [https://doi.org/10.1016/S0260-8774\(00\)00205-3](https://doi.org/10.1016/S0260-8774(00)00205-3)
- Chen, D., Li, M., & Zhu, X. (2012). TG-DSC method applied to drying characteristics and heat requirement of cotton stalk during drying. *Heat and Mass Transfer*, 48(12), 2087–2094. <https://doi.org/10.1007/s00231-012-1050-6>
- Chen, H., Marks, B. P., & Murphy, R. Y. (1999). Modeling coupled heat and mass transfer for convection cooking of chicken patties. *Journal of Food Engineering*, 42(3), 139–146. [https://doi.org/10.1016/S0260-8774\(99\)00111-9](https://doi.org/10.1016/S0260-8774(99)00111-9)
- Chen, Q., Bi, J., Wu, X., Yi, J., Zhou, L., & Zhou, Y. (2015). Drying kinetics and quality attributes of jujube (*Zizyphus jujuba* Miller) slices dried by hot-air and short- and medium-wave infrared radiation. *LWT - Food Science and Technology*, 64(2), 759–766. <https://doi.org/10.1016/j.lwt.2015.06.071>
- Chua, K. J., & Chou, S. K. (2003). Low-cost drying methods for developing countries. *Trends in Food Science & Technology*, 14(12), 519–528. <https://doi.org/10.1016/j.tifs.2003.07.003>
- COMSOL (n.d.). MultiPhysics 5.4. Convection Cooking of Chicken Patties. https://www.comsol.com/model/download/541551/models.heat.chicken_patties.pdf
- Condori, M., Echazú, R., & Saravia, L. (2001). Solar drying of sweet pepper and garlic using the tunnel greenhouse drier. *Renewable Energy*, 22(4), 447–460. [https://doi.org/10.1016/S0960-1481\(00\)00098-7](https://doi.org/10.1016/S0960-1481(00)00098-7)
- da Silva, W. P., e Silva, C. M. D. P. S., & Gomes, J. P. (2013). Drying description of cylindrical pieces of bananas in different temperatures using diffusion models. *Journal of Food Engineering*, 117(3), 417–424. <https://doi.org/10.1016/j.jfoodeng.2013.03.030>
- de Lima, A. G. B., Farias Neto, S. R., & Silva, W. P. (2012). Heat and mass transfer in porous materials with complex geometry: Fundamentals and applications. In: J. Delgado (Ed.), *Heat and Mass Transfer in Porous Media*. Advanced Structured Materials (Vol. 13). Berlin, Heidelberg: Springer. https://doi.org/10.1007/978-3-642-21966-5_7
- de Lima, A. G. B., Queiroz, M. R., & Nebra, S. A. (2002). Simultaneous moisture transport and shrinkage during drying of solids with ellipsoidal configuration. *Chemical Engineering Journal*, 86(1), 85–93. [https://doi.org/10.1016/S1385-8947\(01\)00276-5](https://doi.org/10.1016/S1385-8947(01)00276-5)
- de Souza, L. F., de Andrade, E. T., & Rios, P. d. A. (2019). Determination of volumetric contraction and drying kinetics of the dried banana. *Theoretical and Applied Engineering*, 3(1), 20–30. <https://doi.org/10.31422/tae.v2i4.10>
- Department of Agricultural Extension. (n.d.). Information System for Agricultural Production. Retrieved from <http://www.doae.go.th>
- Dondee, S., Meeso, N., Soponronnarit, S., & Siriamornpun, S. (2011). Reducing cracking and breakage of soybean grains under combined near-infrared radiation and fluidized-bed drying. *Journal of Food Engineering*, 104(1), 6–13. <https://doi.org/10.1016/j.jfoodeng.2010.11.018>
- Farias, R. P., Gomez, R. S., Silva, W. P., Silva, L. P. L., Oliveira Neto, G. L., Santos, I. B., ... Lima, A. G. B. (2020). Heat and mass transfer, and volume variations in banana slices during convective hot air drying: An experimental analysis. *Agriculture*, 10(10), 423. <https://doi.org/10.3390/agriculture10100423>
- Gluannec, P., Lecharpentier, D., & Noel, H. (2002). Experimental survey on the combination of radiating infrared and microwave sources for the drying of porous material. *Applied Thermal Engineering*, 22(15), 1689–1703. [https://doi.org/10.1016/S1359-4311\(02\)00071-6](https://doi.org/10.1016/S1359-4311(02)00071-6)
- Hebbbar, H. U., Vishwanathan, K. H., & Ramesh, M. N. (2004). Development of combined infrared and hot air dryer for vegetables. *Journal of Food Engineering*, 65(4), 557–563. <https://doi.org/10.1016/j.jfoodeng.2004.02.020>
- Horuz, E., & Maskan, M. (2015). Hot air and microwave drying of pomegranate (*Punica granatum* L.) arils. *Journal of Food Science and Technology*, 52(1), 285–293. <https://doi.org/10.1007/s13197-013-1032-9>

- Jain, D., & Pathare, P. B. (2007). Study the drying kinetics of open sun drying of fish. *Journal of Food Engineering*, 78(4), 1315–1319. <https://doi.org/10.1016/j.jfoodeng.2005.12.044>
- Jamradloedluk, J., Nathakaranakule, A., Soponronnarit, S., & Prachayawarakorn, S. (2007). Influences of drying medium and temperature on drying kinetics and quality attributes of durian chip. *Journal of Food Engineering*, 78(1), 198–205. <https://doi.org/10.1016/j.jfoodeng.2005.09.017>
- Janjai, S., & Tung, P. (2005). Performance of a solar dryer using hot air from roof-integrated solar collectors for drying herbs and spices. *Renewable Energy*, 30(14), 2085–2095. <https://doi.org/10.1016/j.renene.2005.02.006>
- Jindarat, W., Rattanadecho, P., & Vongpradubchai, S. (2011). Analysis of energy consumption in microwave and convective drying process of multi-layered porous material inside a rectangular wave guide. *Experimental Thermal and Fluid Science*, 35(4), 728–737. <https://doi.org/10.1016/j.expthermflusc.2010.11.008>
- Kaveh, M., Golpour, I., Gonçalves, J. C., Ghafouri, S., & Guiné, R. (2021). Determination of drying kinetics, specific energy consumption, shrinkage, and colour properties of pomegranate arils submitted to microwave and convective drying. *Open Agriculture*, 6(1), 230–242. <https://doi.org/10.1515/opag-2020-0209>
- Kipcak, A. S., & Doymaz, I. (2020a). Mathematical modeling and drying characteristics investigation of black mulberry dried by microwave method. *International Journal of Fruit Science*, 20(3), 1222–1233. <https://doi.org/10.1080/15538362.2020.1782805>
- Kipcak, A. S., & Doymaz, I. (2020b). Microwave and infrared drying kinetics and energy consumption of cherry tomatoes. *Chemical Industry & Chemical Engineering Quarterly*, 26(2), 203–212. <https://doi.org/10.2298/CICEQ190916039K>
- Maskan, M. (2000). Microwave/air and microwave finish drying of banana. *Journal of Food Engineering*, 44(2), 71–78. [https://doi.org/10.1016/S0260-8774\(99\)00167-3](https://doi.org/10.1016/S0260-8774(99)00167-3)
- Naknaen, P., Charoenthakij, P., & Kerdsup, P. (2016). Physicochemical properties and nutritional compositions of foamed banana powders (Pisang Awak, *Musa sapientum* L.) dehydrated by various drying methods. *Walailak Journal of Science and Technology*, 13(3), 177–191. <https://doi.org/10.14456/WJST.2016.18>
- Nguyen, M.-H., & Price, W. E. (2007). Air-drying of banana: Influence of experimental parameters, slab thickness, banana maturity and harvesting season. *Journal of Food Engineering*, 79(1), 200–207. <https://doi.org/10.1016/j.jfoodeng.2006.01.063>
- Ning, X., & Han, C. (2013). Drying characteristics and quality of taeguik ginseng (*Panax ginseng* C.A. Meyer) using far-infrared rays. *International Journal of Food Science & Technology*, 48(3), 477–483. <https://doi.org/10.1111/j.1365-2621.2012.03208.x>
- Pan, Z., & Atungulu, G. (2010). *Infrared heating for food and agricultural processing*. Boca Raton, FL: CRC Press.
- Pianroj, Y., Werapun, W., Inthapan, J., Jumrat, S., & Karrila, S. (2018). Mathematical modeling of drying kinetics and property investigation of natural crepe rubber sheets dried with infrared radiation and hot air. *Drying Technology*, 36(12), 1436–1445. <https://doi.org/10.1080/07373937.2017.1407939>
- Prachayawarakorn, S., Tia, W., Plyto, N., & Soponronnarit, S. (2008). Drying kinetics and quality attributes of low-fat banana slices dried at high temperature. *Journal of Food Engineering*, 85(4), 509–517. <https://doi.org/10.1016/j.jfoodeng.2007.08.011>
- Puangsuwan, K., Chongcheawchamnan, M., & Tongura, C. (2015). Effective moisture diffusivity, activation energy and dielectric model for palm fruit using a microwave heating. *Journal of Microwave Power and Electromagnetic Energy*, 49(2), 100–111. <https://doi.org/10.1080/08327823.2015.11689900>
- Puangsuwan, K., Wongsopanukul, K., Tongurai, C., Channumsin, S., Sreesawet, S., & Chongcheawchamnan, M. (2021). Pretreatment of palm fruit by using a conveyor belt microwave prototype. *Engineering Journal*, 25(1), 33–41. <https://doi.org/10.4186/ej.2021.25.1.33>
- Rahman, M. H., Ahmed, M. W., & Islam, M. N. (2018). Drying kinetics and sorption behavior of two varieties banana (sagor and sabri) of Bangladesh. *SAARC Journal of Agriculture*, 16(2), 181–193. <https://doi.org/10.3329/sja.v16i2.40269>
- Robinson, J. C., & Galan Saucó, V. (2011). *Bananas and plantains*. Wallingford: CABI.
- Sakai, N., & Hanzawa, T. (1994). Applications and advances in far-infrared heating in Japan. *Trends in Food Science & Technology*, 5(11), 357–362. [https://doi.org/10.1016/0924-2244\(94\)90213-5](https://doi.org/10.1016/0924-2244(94)90213-5)
- Salehi, F., Kashaninejad, M., & Jafarianlari, A. (2017). Drying kinetics and characteristics of combined infrared-vacuum drying of button mushroom slices. *Heat and Mass Transfer*, 53(5), 1751–1759. <https://doi.org/10.1007/s00231-016-1931-1>
- Sankat, C. K., & Castaigne, F. (2004). Foaming and drying behaviour of ripe bananas. *LWT – Food Science and Technology*, 37(5), 517–525. [https://doi.org/10.1016/S0023-6438\(03\)00132-4](https://doi.org/10.1016/S0023-6438(03)00132-4)
- Seyedabadi, E., Khojastehpour, M., & Abbaspour-Fard, M. H. (2017). Convective drying simulation of banana slabs considering non-isotropic shrinkage using FEM with the arbitrary Lagrangian–Eulerian method. *International Journal of Food Properties*, 20(Suppl 1), S36–S49. <https://doi.org/10.1080/10942912.2017.1288134>
- Singh, R. P., & Heldman, D. R. (2014). *Introduction to food engineering*. Amsterdam: Elsevier.
- Smitabhindu, R., Janjai, S., & Chankong, V. (2008). Optimization of a solar-assisted drying system for drying bananas. *Renewable Energy*, 33(7), 1523–1531. <https://doi.org/10.1016/j.renene.2007.09.021>
- Sungsoontorn, S., Jumrat, S., Pianroj, Y., & Rattanadecho, P. (2016). Design and analysis of a doubly corrugated filter for a combined multi-feed microwave-hot air and continuous belt system. *Songklanakarin Journal of Science and Technology*, 38(4), 337–379. <https://doi.org/10.14456/sjst-psu.2016.49>
- Thuwapanichayanan, R., Prachayawarakorn, S., & Soponronnarit, S. (2008). Drying characteristics and quality of banana foam mat. *Journal of Food Engineering*, 86(4), 573–583. <https://doi.org/10.1016/j.jfoodeng.2007.11.008>
- Tirawanichakul, S., Na Phatthalung, W., & Tirawanichakul, Y. (2008). Drying strategy of shrimp using hot air convection and hybrid infrared radiation/hot air convection. *Walailak Journal of Science and Technology*, 5(1), 77–100.
- Tunckal, C., & Doymaz, I. (2020). Performance analysis and mathematical modelling of banana slices in a heat pump drying system. *Renewable Energy*, 150, 918–923. <https://doi.org/10.1016/j.renene.2020.01.040>
- Wang, Z., Sun, J., Liao, X., Chen, F., Zhao, G., Wu, J., & Hu, X. (2007). Mathematical modeling on hot air drying of thin layer apple pomace. *Food Research International*, 40(1), 39–46. <https://doi.org/10.1016/j.foodres.2006.07.017>

How to cite this article: Puangsuwan, K., Jumrat, S., Muangprathub, J., Punvichai, T., Karrila, S., & Pianroj, Y. (2021). Hybrid infrared with hot air drying of Pisang-Awak banana: Kinetics and shrinkage quality. *Journal of Food Process Engineering*, e13827. <https://doi.org/10.1111/jfpe.13827>